The decay mechanism of photoexcited guanine A nonadiabatic dynamics study

Mario Barbatti, Jaroslaw J. Szymczak, Adélia J. A. Aquino, Dana Nachtigallová, and Hans Lischka

Articles you may be interested in

The effect of pressure on the hydration structure around hydrophobic solute: A molecular dynamics simulation study
J. Chem. Phys. **136**, 114510 (2012); 10.1063/1.3694834

Electron paramagnetic resonance study of unpaired electron species in thin films of pyrimidine bases induced by nitrogen and oxygen K-shell photoabsorption
Appl. Phys. Lett. **98**, 103701 (2011); 10.1063/1.3563712

First Principles Dynamics of Photoexcited DNA and RNA Bases
AIP Conf. Proc. **963**, 219 (2007); 10.1063/1.2836045

Ultrafast repair of irradiated DNA: Nonadiabatic ab initio simulations of the guanine-cytosine photocycle
J. Chem. Phys. **126**, 175102 (2007); 10.1063/1.2728897

Nonadiabatic molecular dynamics simulation of photoexcitation experiments for the solvated electron in methanol
J. Chem. Phys. **110**, 10953 (1999); 10.1063/1.479032

The decay mechanism of photoexcited guanine − A nonadiabatic dynamics study

Mario Barbatti,[1,2,a)] Jaroslaw J. Szymczak,[2,b)] Adélia J. A. Aquino,[2] Dana Nachtigallová,[3] and Hans Lischka[2,c)]

[1]*Max-Planck-Institut für Kohlenforschung, Kaiser-Wilhelm-Platz 1, D-45470 Mülheim an der Ruhr, Germany*
[2]*Institute for Theoretical Chemistry - University of Vienna, Waehringerstrasse 17, A 1090 Vienna, Austria*
[3]*Institute of Organic Chemistry and Biochemistry, Academy of Sciences of the Czech Republic, Flemingovo nam. 2, CZ-16610 Prague 6, Czech Republic*

Ab initio surface hopping dynamics calculations were performed for the biologically relevant tautomer of guanine in gas phase excited into the first $\pi\pi^*$ state. The results show that the complete population of UV-excited molecules returns to the ground state following an exponential decay within ∼220 fs. This value is in good agreement with the experimentally obtained decay times of 148 and 360 fs. No fraction of the population remains trapped in the excited states. The internal conversion occurs in the $\pi\pi^*$ state at two related types of conical intersections strongly puckered at the C2 atom. Only a small population of about 5% following an alternative pathway via a $n\pi^*$ state was found in the dynamics. © *2011 American Institute of Physics*. [doi:10.1063/1.3521498]

I. INTRODUCTION

Like the four other natural nucleobases, UV-excited guanine shows ultrafast radiationless deactivation in gas phase with a decay time of a few picoseconds in the maximum,[1–3] which implies that it returns to the ground state by means of an internal conversion mechanism. These ultrafast deactivation mechanisms of guanine and of the other nucleobases and their related photostability are of great interest since they are considered to contribute to a natural chemical defense of the genetic code against damaging photochemically induced processes in reactive excited states.[4]

The guanine deactivation processes have been measured at 267 nm pump wavelength,[1–3] slightly below the center of the first absorption band (284 nm).[5] The exact time constants depend on the details of the experimental setup and on the way of the transient spectra are analyzed. When only the non-fragmented guanine channel is included in the analysis of the transient spectrum, guanine deactivation has been explained by two time constants of 0.148 and 0.36 ps.[2] When, however, fragment mass channels are included as well, the longer time constant has been found to increase more than six times to 2.3 ps.[3]
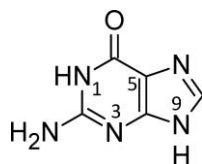
SCHEME 1.

Three main reaction pathways have been identified computationally for internal conversion of guanine (9H-1H-keto-guanine, Scheme 1) from the first $\pi\pi^*$ state to the ground state. The first one is a barrierless pathway with the electronic state characterized as $\pi\pi^*$ excitation and the nuclear motion described by puckering of the C2 atom and displacement of the amino group out of the ring plane.[6–10] Two slightly different kinds of conical intersections (denoted *ethylenic I* and *ethylenic II*) can be accessed through this pathway. The second pathway leads to a conical intersection characterized by puckering of the C6 atom and displacement of the oxygen atom out of the ring plane.[6–8] The third alternative is characterized by stretching of one of the NH bonds, promoting an intersection of the $\pi\sigma^*$ state with the ground state. Reference 9 shows that this pathway may contribute to the deactivation for excitation energies around 0.4 eV above the absorption maximum of the first bright $\pi\pi^*$ state. In the present, work we concentrated on a narrower range of excitation energies below values relevant to N-H dissociation and, therefore, did not consider this reaction channel further.

The guanine decay dynamics (see Ref. 2 and discussion above) has been interpreted by Serrano-Andrés *et al.*[7] by a three-state model based on computed minimum energy paths. The fast decay time observed experimentally (0.148 fs) has been assigned to a direct decay path to the first type of conical intersection (*ethylenic II*), whereas for the explanation of the longer decay time (360 fs) another alternative passing through the S$_1$ $n\pi^*$ minimum has been suggested. Such specific assignments based on static calculations alone are difficult. Dynamics simulations are certainly the appropriate tool to resolve such mechanistic alternatives directly.

So far, non-adiabatic dynamics simulations for excited guanine have been performed with potential energy surfaces computed only with restricted open-shell Kohn–Sham (ROKS)[11] and semi-empirical OM2/MRCI[8] methods, predicting strongly differing results. The ROKS simulations for 9-methyl-guanine and 7-methyl-guanine do not show the involvement of conical intersections. Instead, the internal

a)Electronic mail: barbatti@mpi-muelheim.mpg.de.
b)Electronic mail: jaroslaw.szymczak@univie.ac.at.
c)Electronic mail: hans.lischka@univie.ac.at.

TABLE I. Vertical excitation energies (eV) and oscillator strengths (in parenthesis) for guanine.

Geometry	State	Excitation[a]	MR-CIS	CASPT2 (Ref. 9)	CASPT2 (Ref. 7)	CC2 (Ref. 24)
Min S_0	S_0	cs	0.00	0.00	0.00	0.00
	S_1	$\pi\pi^*$	5.82 (0.158)	4.51 (0.164)	4.93 (0.158)	4.98 (0.132)
	S_2	π-3s		4.89 (0.005)		5.08 (0.028)
	S_3	$n\pi^*$	5.89 (0.007)	5.22 (0.001)	5.54 (0.002)	5.38 (0.003)

[a]cs—closed shell.

conversion is predicted to occur by means of weak couplings induced by out-of-plane vibrational motions around the excited state minimum with a lifetime estimated to be in the range from 0.7 to 8.1 ps for 9-methyl-guanine.[11] The semi-empirical simulations predict that the $S_1 \rightarrow S_0$ deactivation proceeds via two types of conical intersections occurring along the $\pi\pi^*$ pathway with time constants of 0.19 and 0.4 ps.[8] In recent years nonadiabtic simulations based on *ab initio* methods [complete active space self-consistent field (CASSCF) and multireference configuration interaction (MRCI)] have become available and have been applied to calculations on nucleobases and related compounds.[12,13] In the present study simulations are performed on the photostability of guanine using extended *ab initio* methods based on the MRCI method in the framework of the on-the-fly surface-hopping dynamics approach to get better insight into the deactivation mechanism and decay times of this molecule.

II. COMPUTATIONAL DETAILS

Energies, energy gradients and nonadiabatic couplings used in the nonadiabatic dynamics simulations were computed at the multireference configuration interaction level including single excitations (MR-CIS). Molecular orbitals were determined at the state-averaged (SA)-CASSCF level employing a space composed of 12 active electrons in nine orbitals [CAS(12,9)]. At the ground state minimum, this space consists of five π, one n_O, and three π^* orbitals. State averaging was performed over three states (SA-3). The reference space for the MR-CIS calculation was composed of 10 electrons in seven orbitals. A total of 22 orbitals were kept in the frozen core. The 6-31G* basis set was employed for all atoms. Analytical energy gradients and nonadiabatic coupling vectors were computed by the procedures described in Ref. 14. Cartesian coordinates for the minima and conical intersections optimized at this level are given in the supplementary material.[15]

Dynamics simulations were performed with the fewest switches surface hopping approach.[16] Sixty trajectories were computed for a maximum of 600 fs. Trajectories that returned to the ground state and stayed there for more than 100 fs were terminated. The classical equations were integrated with the Velocity-Verlet algorithm[17] using a 0.5 fs time step. The quantum equations were integrated with the 5th-order Butcher algorithm[18] with a 0.01 fs time step using linear interpolation between the time steps of the classical dynamics. Decoherence corrections with $\alpha = 0.1$ hartree were applied.[19] Initial conditions were generated based on a Wigner distribution for the harmonic oscillator as described in Refs. 20 and 21. Trajectories where initiated in a restricted spectral window at the

calculated band maximum (5.62 ± 0.25 eV). In this window the bright state distributes its intensity as 64% for the S_1 state and 36% for the S_2 state. To approximately keep this proportion, 38 and 22 trajectories were initiated in the $\pi\pi^*$ state belonging to the S_1 and S_2 states, respectively.

The dynamics simulations were performed using the NEWTON-X program[22] interfaced with the COLUMBUS[23] program package.

III. RESULTS AND DISCUSSION

A. Potential energy surfaces

The lowest vertical excitation energies and the corresponding oscillator strengths computed at the MR-CIS level are shown in Table I along with benchmark results computed with the CASPT2[7,9] and RI-CC2[24] methods. For all methods, the S_1 state has $\pi\pi^*$ character and it is closely followed by a dark $n\pi^*$ state. When basis sets augmented by diffuse functions are employed, the π-3s state appears in between. A detailed discussion on the guanine spectrum can be found in Refs. 20 and 24 and references therein. As expected, the MR-CIS level produces a $\pi\pi^*$ excitation energy that is too high compared to the higher correlated methods. Besides that, the S_1 minimum ($n\pi^*$) is also somewhat displaced to higher energies at MR-CIS level (4.86 eV) in comparison to the CASPT2 results [4.0 eV (Ref. 7) and 4.55 eV (Ref. 10)]. The energies of the conical intersections between the ground and the first excited states are in quite good agreement with the CASPT2 results of Ref. 7 as discussed next.

A number of conical intersections between the first excited state and the ground state have been reported for guanine.[6–10] Geometric and energetic characterization of present and previous results is provided in Table II. Since most of the intersection structures are highly ring puckered, the Cremer–Pople (CP) parameters[25] together with the Boeyens conformer classification[26] are used for their analysis. The CP parameter Q indicates the degree of ring puckering, where Q = 0 Å indicates planar structures. The additional CP parameters θ and ϕ indicate the kind of ring puckering, which can be classified[26] as boat (B), envelope (E), chair (C), half-chair (H), screw-boat (S), and twisted-boat (T) as shown in Fig. 1.

The investigated conical intersections are grouped into three classes as shown in Table II and Fig. 2. The first type of conical intersections is characterized by ring deformation at the C2 atom with strong out-of-plane distortion of the amino group. It was first reported in Refs. 6–8 and has an envelope conformation puckered at C2 (E_2 conformation). It is characterized as crossing between the $\pi\pi^*$ and the closed shell

TABLE II. Characterization of the S_1/S_0 conical intersections of guanine in terms of the S_1/S_0 energies, the Cremer–Pople parameters Q, θ, and ϕ and of the N10C2N1C6 angle δ (degrees) and the bond N1C6 distance ρ (Å).

	Crossing	Energy (eV)	Q (Å)	θ (°)	ϕ (°)	Conf.	Other features	Methods	Ref.
Ethylenic I	$\pi\pi$*/cs	4.07	0.51	58	58	E_2	$\delta = 80°$	MR-CIS	[b]
		4.1	0.49	60	67	E_2	$\delta = 83°$	CASPT2//CASSCF	[7]
Ethylenic II	$\pi\pi$*/cs	4.30	0.65	73	61	$B_{2,5}$	$\delta = 144°$	MR-CIS	[b]
		4.3	0.61	71	59	E_2	$\delta = 140°$	CASPT2//CASSCF	[7]
		3.4	0.66	81	67	$B_{2,5}$	$\delta = 153°$	CASPT2//CASSCF	[9]
		3.4	0.69	72	56	E_2	$\delta = 143°$	CASPT2//CASSCF	[9]
oop-O	$(\pi+n_O)\pi_O$*/cs	4.45	0.61	58	332	$^1S_6$	$\rho = 2.07$	MR-CIS	[b]
		4.0	0.44	51	328	$^1H_6$	$\rho = 1.85$	CASPT2//CASSCF	[7]

[a]cs—closed shell.
[b]Present work.

(cs) states and is analogous to the intersections found in ethylene and substituted ethylenes.[27] For this reason it is termed *ethylenic I* conical intersection (see also Fig. 2). A second kind of conical intersection also puckered at C2 has been reported in Refs. 7, 9, and 10. Its geometry has an E_2 conformation according to Refs. 7 and 9. Since this type of crossing occurs also between the $\pi\pi$* and closed shell states caused by twisted bonds, it is labeled *ethylenic II* intersection. In Ref. 9. another conical intersection additionally puckered at C5 ($B_{2,5}$) has been found. Following the dihedral angle criterion discussed in the next paragraph, it can also be classified as an *ethylenic II* conical intersection.

The main geometrical difference between *ethylenic I* and *ethylenic II* intersections is found in the position of the amino group. In the first case the dihedral angle between atoms N10, C2, N1, and C6 atoms is about 80° to 90°, which means that the amino group is approximately perpendicular to the ring plane. In the second case, the same dihedral angle assumes values of about 140° to 150°, which puts the amino group pointing nearly parallel to the ring plane. Serrano-Andres and co-workers[7] have shown that the *ethylenic I* and *ethylenic II* conical intersections are connected by the same branch of crossing seam. Since the $\pi\pi$* pathway directly connects the Franck–Condon region to the *ethylenic II* intersection, they concluded that this conical intersection should be the photochemically relevant structure in guanine. We shall return to this point when discussing the dynamics results.

The third type of conical intersections (Fig. 2) is puckered at C6 and has the oxygen atom strongly distorted out of the ring plane.[6–8] For this reason it is called *oop-O* conical intersection. Another geometrical feature of these inter-

sections is the large N1C6 bond distance. The *oop-O* intersections correspond to a crossing between the $\pi\pi_O$*, $n_O\pi_O$*, and the cs configurations. Lan *et al.*[8] have also reported a conical intersection characterized by strong C2N3 stretching and puckering at the C5 and C6 atoms. This intersection does not contain twisted bonds like the *ethylenic* intersections, but it seems to be analogous to the stretched conical intersection observed in the methaniminium cation.[27] In spite of several attempts, an intersection with such features could not be located at the MR-CIS level. It has also not been reported in previous CASSCF/CASPT2 investigations.[7, 9]

B. Dynamics simulations results

The time evolution of the state occupations is shown in Fig. 3. At the initial time the trajectories were distributed in a ratio ∼6:4 between the S_1 and the S_2 states. The S_2 state is quickly depopulated within 20 fs and a corresponding increase in the S_1 population (Fig. 3, top) is observed. At about 100 fs, the S_1 state starts to transfer the population to the ground state. The time evolution of the S_0 population is characterized by fitting the total excited-state population with the function

$$f(t) = f_0 + (1 - f_0)\exp(-(t - t_c)/t_d), \qquad (1)$$
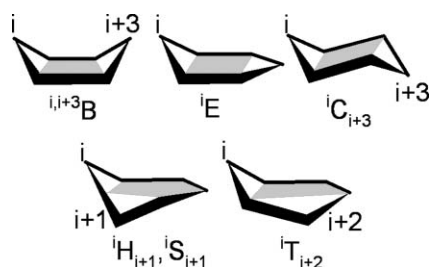
FIG. 1. Schematic representation of the ring puckering conformations according to the Boeyens classification.[26]
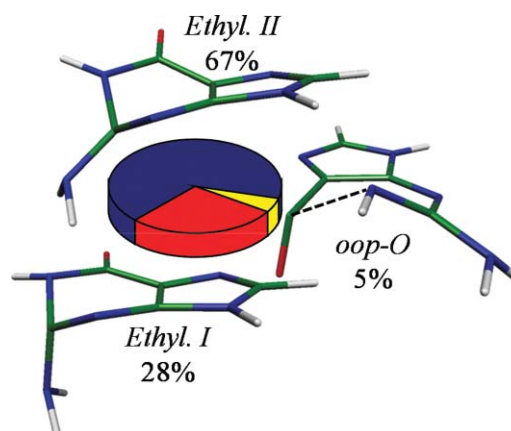
FIG. 2. Three of the main conical S_1/S_0 intersections of guanine. The percentages indicate how often each type of structure is accessed for deactivation in the present dynamics simulations.
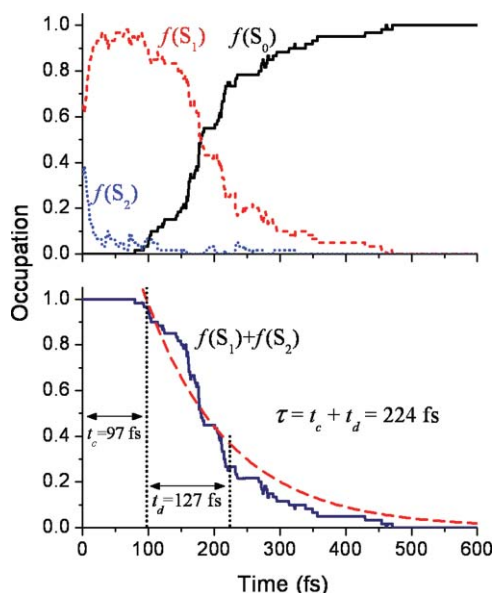
FIG. 3. Time evolution of the occupation of the S_0, S_1, and S_2 states (top). Time evolution of the total excited state occupation together with the fitting parameters (bottom).

where f_0 is the fraction of the population which does not deactivate to the ground state, t_d is the exponential time constant and t_c is the time to initiate the transfer to the ground state. The excited-state life time is given by $\tau = t_c + t_d$. The fitting process results in $f_0 = 0$, $t_c = 97$ fs, $t_d = 127$ fs, and $\tau = 224$ fs (Fig. 3, bottom). These data show that the whole population deactivates with a single time constant and that no remaining fraction is left to deactivate at longer time scales.

The Cremer–Pople parameters θ and ϕ for the $S_1 \rightarrow S_0$ hopping structures are displayed in Fig. 4. The hopping events occur at a very restricted section of the θ-ϕ space, near the E_2 conformation. These structures correspond to *ethylenic* conical intersections. Most of hops occur at strongly distorted ring structures. In 59% of the cases the ring plane was puckered by more than $Q = 0.6$ Å. 18% of the hopping events occurred for
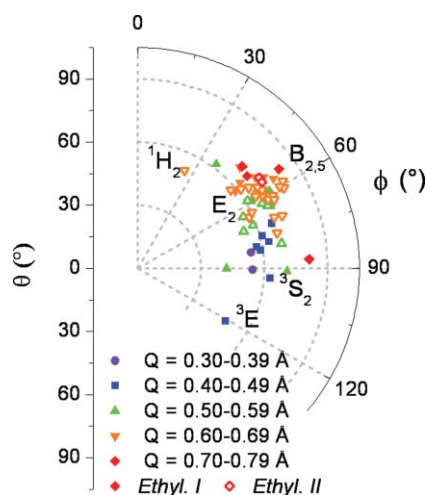

FIG. 4. Cremer–Pople parameters for the $S_1 \rightarrow S_0$ hopping structures. Open symbols indicate *ethylenic I* structures. Full symbols indicate *ethylenic II* structures.

ring distortions between $Q = 0.3$ and 0.5 Å. From Fig. 4 it can be seen that in these cases the ring deformation also involved out-of-plane deformation of the N3 atom and that they are mostly associated with *ethylenic I* structures.

The analysis of the structures at the hopping time shows that *ethylenic II* intersections are accessed in 67% of trajectories (see Fig. 2). *Ethylenic I* intersections are accessed only in 28% of trajectories. In both cases, the trajectories follow exclusively the $\pi\pi^*$ state until hopping to the ground state occurs. No significant difference in the lifetime of each group can be observed. In the remaining 5% of trajectories the deactivation occurred in *oop-O* intersections. The few trajectories that deactivated at this type of conical intersection first relaxed to the $n_O\pi^*$ minimum.

The predominance of the *ethylenic II* conical intersection for guanine deactivation is in agreement with the analysis of Ref. 7, which — based on reaction pathways—predicted that this conical intersection should be the photochemically most relevant one. The present dynamics results show, however, that also the *ethylenic I* conical intersection is accessed for deactivation by a non-negligible fraction of the excited-state population.

The semi-empirical dynamics simulations of Ref. 8 also showed dominance of the $\pi\pi^*$ pathway with a similar lifetime. Nevertheless, most of deactivation reported in that work (60%) occurred at the C2N3 stretched conical intersection, which, as discussed in the previous section, does not seem to exist at the MR-CIS level. The other 40% of the deactivation occurred at the *ethylenic I* conical intersection, in qualitative agreement with our results (28%).

The geometric structures of the *ethylenic* conical intersections do not show fragmentation or bond rearrangements. Therefore, the dominant deactivation at these intersections should mostly correspond to photophysical processes maintaining the guanine structure. In this case, the computed lifetime (0.224 ps) should be compared to the experimental time constants of the nonfragmented channel (0.148, 0.36 ps). Explicit time-resolved simulations of the ionization probability similar to the ones performed by Hudock *et al.*[13] would be necessary for direct comparison with the experimentally determined decay times. Keeping this in mind the computed decay time and the experimental data are in quite good agreement.

IV. CONCLUSIONS

Nonadiabatic dynamics simulations were performed for the biologically relevant tautomer of guanine in gas phase at a flexible *ab initio* multireference (MR-CIS) level. Starting in the first bright $\pi\pi^*$ state (either S_1 and S_2), the deactivation to the ground state takes place in about 224 fs which can be well-described by a single-exponential decay pattern. It is also important to note that the structural distribution of the hopping geometries is quite homogenous. Most of trajectories (95%) followed a $\pi\pi^*$ reaction pathway which reaches the S_1/S_0 crossing seam at geometries strongly puckered at the C2 atom with the amino group distorted out of the ring plane. The remaining trajectories (5%) returned to the ground

state via another puckering at the C6 atom, strong N1C6 stretching and displacement of the oxygen atom out of the ring plane. These results definitely show that also for guanine the decay proceeds via conical intersections and not via vibronic coupling as reported from ROKS calculations[11] on the related 9-methyl-guanine. The previous semiempirical OM2 calculations[8] agree with our result in terms of the predicted $\pi\pi^*$ pathway, for the actual pathway significant deviations to our findings are observed.

The simulated deactivation time is in good agreement with the experimental range of deactivation times obtained for nonfragmented products in the transient signal. This, together with fact that all studied trajectories returned to the ground state within the simulation time (600 fs) implies that the longer time constant of 2.3 ps reported for guanine[3] does not fit the biologically relevant guanine tautomer. Our dynamics simulations also show that for the photo decay initiated in the first $\pi\pi^*$ state practically only one excited state—always of $\pi\pi^*$ character—is involved and that the suggested second pathway passing through a $n\pi^*$ state[7] is not considered important due to its relatively small probability of 5%.

ACKNOWLEDGMENTS

[1] H. Kang, K. T. Lee, B. Jung, Y. J. Ko, and S. K. Kim, J. Am. Chem. Soc. **124**, 12958 (2002).

[2] C. Canuel, M. Mons, F. Piuzzi, B. Tardivel, I. Dimicoli, and M. Elhanine, J. Chem. Phys. **122**, 074316 (2005).

[3] M. Mons, I. Dimicoli, and F. Piuzzi, in *Radiation Induced Molecular Phenomena in Nucleic Acids*, edited by M. K. Shukla and J. Leszczynski (Springer Netherlands, 2008), pp. 343.

[4] L. Serrano-Andres and M. Merchan, J. Photochem. Photobiol. C-Photochem. Rev. **10**, 21 (2009).

[5] L. B. Clark, G. G. Peschel, and I. Tinoco, J. Phys. Chem. **69**, 3615 (1965).

[6] C. M. Marian, J. Phys. Chem. A **111**, 1545 (2007).

[7] L. Serrano-Andres, M. Merchan, and A. C. Borin, J. Am. Chem. Soc. **130**, 2473 (2008).

[8] Z. G. Lan, E. Fabiano, and W. Thiel, Chemphyschem **10**, 1225 (2009).

[9] S. Yamazaki, W. Domcke, and A. L. Sobolewski, J. Phys. Chem. A **112**, 11965 (2008).

[10] H. Chen and S. H. Li, J. Chem. Phys. **124**, 154315 (2006).

[11] H. Langer and N. L. Doltsinis, Phys. Chem. Chem. Phys. **6**, 2742 (2004).

[12] M. Barbatti and H. Lischka, J. Phys. Chem. A **111**, 2852 (2007); M. Barbatti and H. Lischka, J. Am. Chem. Soc. **130**, 6831 (2008); J. J. Szymczak, M. Barbatti, J. T. Soo Hoo, J. A. Adkins, T. L. Windus, D. Nachtigallova, and H. Lischka, J. Phys. Chem. A **113**, 12686 (2009); H. R. Hudock and T. J. Martinez, ChemPhysChem **9**, 2486 (2008).

[13] H. R. Hudock, B. G. Levine, A. L. Thompson, H. Satzger, D. Townsend, N. Gador, S. Ullrich, A. Stolow, and T. J. Martinez, J. Phys. Chem. A **111**, 8500 (2007).

[14] R. Shepard, H. Lischka, P. G. Szalay, T. Kovar, and M. Ernzerhof, J. Chem. Phys. **96**, 2085 (1992); R. Shepard, in *Modern Electronic Structure Theory*, edited by D. R. Yarkony (World Scientific, Singapore, 1995), Vol. 1, pp. 345; H. Lischka, M. Dallos, and R. Shepard, Molecular Physics **100**, 1647 (2002); H. Lischka, M. Dallos, P. G. Szalay, D. R. Yarkony, and R. Shepard, J. Chem. Phys. **120**, 7322 (2004); M. Dallos, H. Lischka, R. Shepard, D. R. Yarkony, and P. G. Szalay, J. Chem. Phys. **120**, 7330 (2004).

[15] See supplementary material at http://dx.doi.org/10.1063/1.3521498 for Cartesian coordinates for the minima and conical intersections optimized at MRCIS/6–31G* level.

[16] J. C. Tully, J. Chem. Phys. **93**, 1061 (1990).

[17] W. C. Swope, H. C. Andersen, P. H. Berens, and K. R. Wilson, J. Chem. Phys. **76**, 637 (1982).

[18] J. Butcher, J. Assoc. Comput. Mach. **12**, 124 (1965).

[19] G. Granucci and M. Persico, J. Chem. Phys. **126**, 134114 (2007).

[20] M. Barbatti, A. J. A. Aquino, and H. Lischka, Phys. Chem. Chem. Phys. **12**, 4959 (2010).

[21] M. Barbatti, J. Pittner, M. Pederzoli, U. Werner, R. Mitric, V. Bonacic-Koutecký, and H. Lischka, Chem. Phys. **375**, 26 (2010).

[22] M. Barbatti, G. Granucci, H. Lischka, M. Ruckenbauer, and M. Persico, NEWTON-X: a package for Newtonian dynamics close to the crossing seam, version 0.14b, www.univie.ac.at/newtonx (2007); M. Barbatti, G. Granucci, M. Persico, M. Ruckenbauer, M. Vazdar, M. Eckert-Maksic, and H. Lischka, J. Photochem. Photobiol. A: Chemistry **190**, 228 (2007).

[23] H. Lischka, R. Shepard, F. B. Brown, and I. Shavitt, Int. J. Quantum Chem. **S15**, 91 (1981); H. Lischka, R. Shepard, R. M. Pitzer, I. Shavitt, M. Dallos, T. Müller, P. G. Szalay, G. S. Kedziora, S. Yabushita, and Z. Y. Zhang, Phys. Chem. Chem. Phys. **3**, 664 (2001); H. Lischka, R. Shepard, I. Shavitt, R. M. Pitzer, M. Dallos, T. Müller, P. G. Szalay, F. B. Brown, R. Ahlrichs, H. J. Boehm, A. Chang, D. C. Comeau, R. Gdanitz, H. Dachsel, C. Ehrhardt, M. Ernzerhof, P. Höchtl, S. Irle, G. Kedziora, T. Kovar, V. Parasuk, M. J. M. Pepper, P. Scharf, H. Schiffer, M. Schindler, M. Schüler, M. Seth, E. A. Stahlberg, J.-G. Zhao, S. Yabushita, Z. Zhang, M. Barbatti, S. Matsika, M. Schuurmann, D. R. Yarkony, S. R. Brozell, E. V. Beck, J.-P. Blaudeau, M. Ruckenbauer, B. Sellner, F. Plasser, and J. J. Szymczak, COLUMBUS, an *ab initio* electronic structure program, release 5.9.2, www.univie.ac.at/columbus (2008).

[24] T. Fleig, S. Knecht, and C. Hattig, J. Phys. Chem. A **111**, 5482 (2007).

[25] D. Cremer and J. A. Pople, J. Am. Chem. Soc. **97**, 1354 (1975).

[26] J. C. A. Boeyens, J. Chem. Crystallogr. **8**, 317 (1978).

[27] M. Barbatti, M. Ruckenbauer, J. J. Szymczak, A. J. A. Aquino, and H. Lischka, Phys. Chem. Chem. Phys. **10**, 482 (2008).